Application of decision analysis to milling profit maximisation: An introduction

Article *in* International Journal of Materials and Product Technology · May 2009

DOI: 10.1504/IJMPT.2009.025220

6 authors, including:

Raul Zapata
United States Navy
20 PUBLICATIONS **81** CITATIONS
SEE PROFILE

Tony L. Schmitz
University of North Carolina at Charlotte
254 PUBLICATIONS **2,714** CITATIONS
SEE PROFILE

Application of decision analysis to milling profit maximisation: an introduction

A.E. Abbas and L. Yang

Department of Industrial and Enterprise Systems Engineering,
University of Illinois at Urbana-Champaign,
117 Transportation Building, MC-238,
Urbana, IL 61801, USA
E-mail: aliabbas@uiuc.edu E-mail: liuyang2@uiuc.edu

R. Zapata and T.L. Schmitz*

Department of Mechanical and Aerospace Engineering,
University of Florida,
237 MAE-B, Gainesville, FL 32611, USA
E-mail: quique@ufl.edu E-mail: tschmitz@ufl.edu
*Corresponding author

Abstract: This paper describes the application of decision analysis to milling optimisation. In this initial study we include the effects of uncertainty in tool life and force model coefficients. The decisions represent the milling operating parameters. A single-attribute value function is used to maximise profit. Stability of the milling operation, surface location error, and surface roughness pose constraints on the feasible decision alternatives. A numerical study comparing four optimisation scenarios is presented where values of tool life and force model coefficients are either deterministic or uncertain. The optimised results are compared to manufacturer recommendations.

Keywords: milling; optimisation; decision analysis; stability lobe diagram; SLE; surface location error.

Reference to this paper should be made as follows: Abbas, A.E., Yang, L., Zapata, R. and Schmitz, T.L. (2009) 'Application of decision analysis to milling profit maximisation: an introduction', *Int. J. Materials and Product Technology*, Vol.

Biographical notes: Ali E. Abbas is an Assistant Professor in the Department of Industrial and Enterprise Systems Engineering at the University of Illinois at Urbana-Champaign. His research interests include decision making under uncertainty, dynamic programming, and information theory. He received his PhD in Management Science and Engineering (2003), and PhD minor in Electrical Engineering from Stanford University. He joined UIUC in 2004, and previously worked as a Lecturer in the Department of Management Science and Engineering at Stanford University and in Schlumberger Oilfield Services. He is a senior member of the IEEE and member of the Decision Analysis Council at INFORMS.

Liu Yang is a PhD student in the Department of Industrial and Enterprise Systems Engineering at the University of Illinois at Urbana-Champaign. He received his BS Degree in Computer Science and Technology in the

University of Science and Technology of China, and received his MS Degree in Computer Software and Theory in the Institute of Computing Technology, Chinese Academy of Sciences. His research interests include decision analysis, game theory, and optimisation, as well as their application to both business and industry.

Raúl Zapata is a PhD student at the Machine Tool Research Center within the University of Florida's Department of Mechanical and Aerospace Engineering. He obtained his BS Degree at the University of Puerto Rico, Mayaguez Campus, and his MS Degree at the University of Florida. His primary research interests are machine tool accuracy and the optimisation of machining process parameter selection.

Tony L. Schmitz is an Associate Professor in the Department of Mechanical and Aerospace Engineering at the University of Florida. His primary interests are in the fields of manufacturing metrology and process dynamics. Prior appointments include a post-doctoral fellowship at the National Institute of Standards and Technology, Gaithersburg, MD, and Lecturer at Johns Hopkins University, Baltimore, MD. Recent professional recognitions include the National Science Foundation CAREER award, Office of Naval Research Young Investigator award, and the Society of Manufacturing Engineers Outstanding Young Manufacturing Engineer award. He received his PhD from the University of Florida in 1999.

1 Introduction

This paper details initial efforts to apply decision analysis to high-speed milling optimisation in the presence of uncertainty. This approach enables the mathematical rigor of decision analysis to be applied to milling optimisation, while taking into account uncertainty in performance prediction. Although both disciplines are well-established, the application of decision analysis specifically to milling optimisation has not been previously realised. For a recent review of decision analysis applications including other manufacturing related issues, we refer the reader to Keefer et al. (2004).

This work does not represent the first attempt at machining optimisation. Previous studies have explored multiple objectives and many optimisation methods; see for example, Gilbert (1950), Okushima and Kitomi (1964), Wu and Ermer (1966), Tee et al. (1969) and Boothroyd and Rusek (1976) for early efforts. In many cases, however, prior studies have focused on a single limitation to milling productivity, such as tool wear. A holistic approach that simultaneously considers multiple restrictions including tool wear, stability (i.e., avoiding chatter, or unstable machining conditions), error in the location of the machined surface due to tool and/or workpiece deflections under stable conditions, and surface finish is required if significant improvements in process performance are to be achieved in general.

Our primary objective in this paper is to present the milling optimisation framework from a decision analytic perspective. In this work we respect limitations imposed by the process dynamics and tool life, while employing a single objective function, profit. The use of profit as the primary objective function whose expected value is to be maximised, while considering the process dynamics, differentiates this work from prior studies on milling optimisation which focused on, for example, maximising tool life

and/or production rate and minimising cost; see, for example, Beightler and Philips (1970), Walvekar and Lambert (1970), Ermer (1971), Hati and Rao (1976), Giardini et al. (1988), Sheikh et al. (1980), Petropoulos (1975), Eskicioglu et al. (1985), Lambert and Walvekar (1978), Jha (1990), Gopalakrishnak and Al-Khayyal (1991), Armarego et al. (1993, 1994), Sonmez et al. (1999), Wang and Armarego (2001), Lin (2002), Kim et al. (2002), Juan et al. (2003) and Lu et al. (2003). In recent work, Deshayes et al. (2005) described robust optimisation efforts within a *Smart Machining System* at the National Institute of Standards and Technology and Tansel et al. (2006) implemented a genetically optimised neural network system to maximise removal rate in micro-endmilling and obtain a best compromise between surface roughness and machining time in mold making.

In this initial work, we maximise profit while considering uncertainty in tool life and cutting Force Model Coefficients (FMC). We discuss the effects of including uncertainty on the optimal milling decisions and present the milling situation as a decision diagram that can be incorporated into software or a decision support system.

The paper is structured as follows. Section 2 provides background information on decision diagrams. We also review the decision variables (parameters) used to describe a milling process design. Section 3 presents

- a deterministic solution to the discretised optimisation problem
- solutions in the presence of uncertainty.

These tasks are demonstrated in the form of a numerical case study. Finally, conclusions and a summary of results are provided.

2 Decision diagram

A decision diagram (Howard and Matheson, 1984, 2005) is a graph-based representation of a decision situation. A decision diagram consists of several nodes with arrows connecting them. There are four types of nodes in a decision diagram: decision, uncertainty, value, and deterministic (see Figure 1).

- A decision node, represented with a rectangle, comprises the set of available alternative for each decision. It may have an underlying structure of a continuous decision variable or a discrete set of alternatives.
- An uncertainty node, represented by an oval, comprises a discrete or continuous uncertain variable in the decision situation. Arrows between the uncertainty nodes represent the relevance (dependence) relations between the variables present.
- A deterministic node represents a deterministic function of its inputs. Deterministic nodes are represented as double ovals in decision diagrams.
- A value node determines the objectives of the decision situation. A value node comprises a value function which determines the value of each instantiation of the outcomes and decision alternatives chosen. Value nodes are usually drawn as a hexagon, octagon, or diamond to differentiate them from regular deterministic nodes.

Figure 1 Nodes in decision diagrams

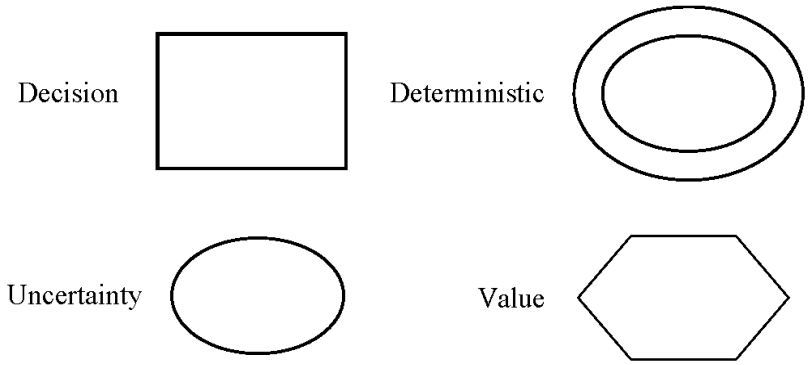

There are several types of arrows in a decision diagram: information, influence, relevance, functional, and direct value; see Figure 2.

- An information arrow is one that leads into a decision node from a either decision or uncertainty node. An information arrow from an uncertainty into a decision node indicates that the outcome of the uncertainty is known before making a decision. An information arrow from a decision node into another decision node is a 'no forgetting' arrow that implies that the decision alternative chosen in the previous decision is recalled.
- An influence arrow is directed from a decision node to an uncertainty node. It indicates that the probability distribution for the uncertainty depends on the selected decision alternative.
- An arrow between two uncertainty nodes is called a relevance arrow. It indicates that the uncertainty probability distribution may be conditional on the other uncertainty.
- An arrow from either an uncertainty node or a decision node into a deterministic node is called a functional arrow. A functional arrow indicates that the deterministic node value is decided by its inputs.
- An arrow from a decision or uncertainty node into the value node is referred to as a direct value arrow.

Figure 2 Arrows in decision diagrams (see online version for colours)

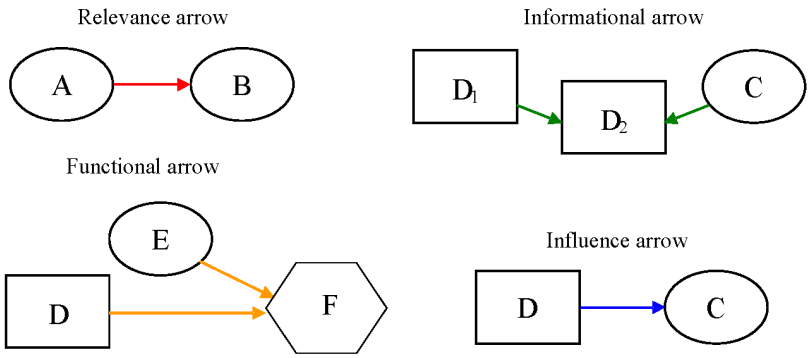

In our formulation, we divide the set of milling decisions to be made into two main categories:

- tool selection
- machining parameter decisions.

These are located in the bottom row of Figure 3 decision diagram. In moving from left to right in Figure 3, we first identify the design node, which contains the work-piece information (material, dimensions, and tolerances) available before any other decisions are made. The tool selection and machining parameter decision nodes follow. Two uncertainty nodes, representing tool life and the FMC (explained in more detail later), are located above the decision nodes. We also include deterministic nodes for: milling process calculations/measurements that depend on the tool selection, machining parameter decisions, and FMC; tool path; and cost and revenue, from which we determine our overall objective function of profit (value node). The corresponding arrows define their connectivity.

- The design node has an arrow to tool selection decisions. However, the design node information is generically available to all subsequent nodes (e.g., the workpiece material influences the tool life and FMC nodes, although an arrow is not explicitly included).
- The tool selection decision node has arrows to the tool life and FMC uncertainty nodes. This is because the tool geometry influences the parameters associated with these models. There are also arrows to milling process calculations/measurements (the tool selection influences the system dynamic response) and the tool path node (the tool selection affects the geometric tool path).
- The machining parameters decision node has arrows to tool life, milling process calculations/measurements, and tool path. In the former two cases, the results of model calculations depend on the parameter decisions. For the latter, the parameters affect the machining time.
- The tool life node has an arrow to cost because the cost equation depends directly on tool life.
- There is an arrow from FMC to milling process calculations/measurements because these coefficients affect process dynamics calculations.
- The milling process calculations/measurements deterministic node has an arrow to cost because the results affect the part quality (i.e., geometric accuracy due to potential Surface Location Error (SLE) and surface roughness).
- There is an arrow from tool path to cost because the machining time is incorporated in the cost equation.
- The cost and revenue nodes have arrows to profit so that it may be calculated.
- Finally, a succession of arrows connects the design, tool selection, machining parameter, and profit nodes to indicate the chronological flow of information.

Figure 3 Decision diagram for machining parameter decisions (radial depth of cut, a; spindle speed, Ω; axial depth of cut, b; and feed per tooth, f_t)

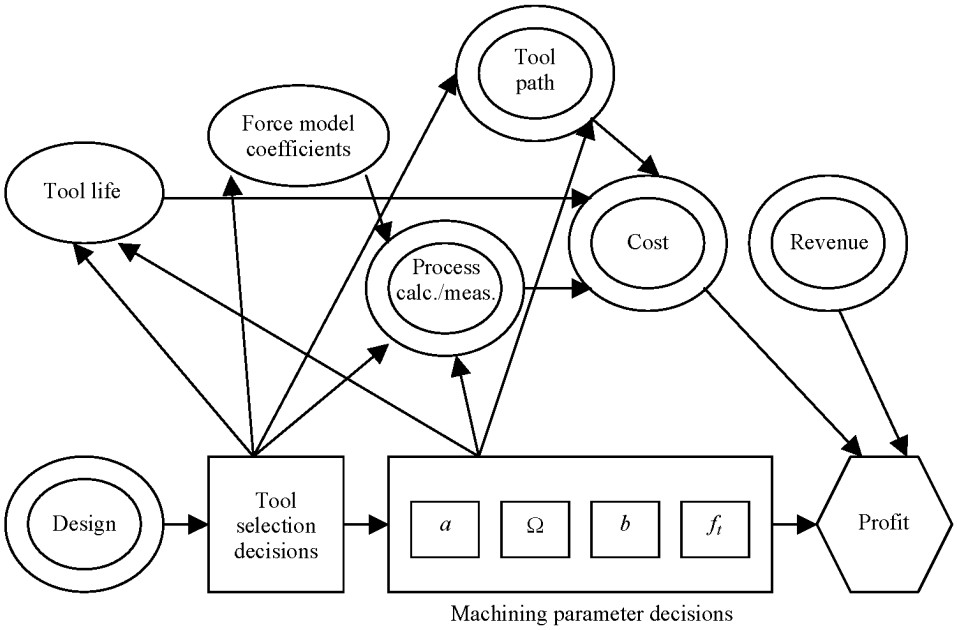

In the following paragraphs we describe the relationships between milling decisions and profit in more detail. We focus on the case where the tool selection decisions are already made for the given design and our goal is to determine the machining parameter decisions. Each of the nodes in Figure 3 decision diagram contains information. Nodes such as axial depth (decision) represent a set of alternatives for the axial depth. The deterministic (milling) process calculations/measurements node, on the other hand, contains a series of equations or numerical procedures used to evaluate specific properties based on the information provided by the input nodes (denoted by arrows pointing to the node). The following sections describe the content of each node to provide a complete understanding of the decision diagram.

2.1 Design

This deterministic node contains all the information that the user knows about the design of the desired part before any machining is performed. It contains the workpiece dimensions, tolerances, required surface finish, and material.

2.2 Tool selection

This decision node contains the tool and holder properties. The tool properties are: tool extension outside the holder (overhang length), number of teeth (flutes), flute length, material, helix angle of the flutes, radius, and teeth runout (variation in radii of the circles traced by the teeth on the rotating tool). The tool holder information includes geometry and material.

2.3 Machining parameter decisions

This group of decision nodes includes values that the user may choose given the information in the design and tool selection nodes. These are: axial depth of cut, radial depth of cut, spindle speed, and feed per tooth. A brief description of each decision (parameter in milling terminology) is now provided.

- Axial depth of cut (b in Figure 4) defines the length of the tool that is engaged in the cut parallel to the rotational axis of the tool. This value cannot exceed the flute length.
- Radial depth of cut (a in Figure 5) defines the cut depth in the radial direction of the endmill (perpendicular to the spindle rotational axis). The radial depth of cut has a maximum value equal to the tool diameter, d, ($a = d$ is referred to as slotting). The radial depth can also be represented as a percentage of the diameter engaged in the cut, referred to as the radial immersion (i.e., slotting is 100% radial immersion).
- Spindle speed describes the speed at which the tool rotates and is usually specified in revolutions per minute, or rpm.
- Feed per tooth (f_t in Figure 6) describes the distance the tool travels in the feed direction between subsequent tooth engagements. A mathematical description is presented in equation (1), where Ω is the spindle speed, N is the number of teeth, and f is the linear feed rate in the feed direction.

$$f_t = \frac{f}{\Omega N}. \tag{1}$$

Figure 4 Axial depth of cut, *b;* the rotational axis of the milling tool is vertical (see online version for colours)

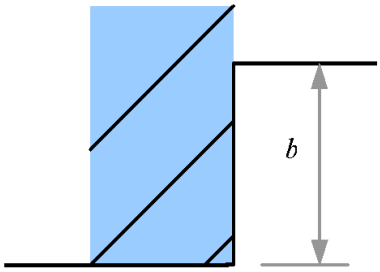

Figure 5 Radial depth of cut, a; the rotating spindle speed, Ω, of the tool is also identified (see online version for colours)

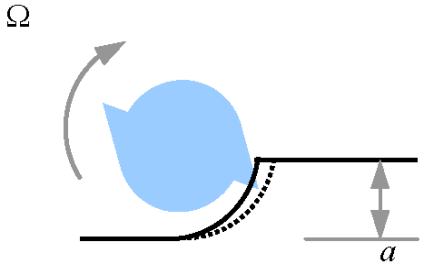

Figure 6 Feed per tooth, f_t; the linear feed rate, f, is also identified (see online version for colours)

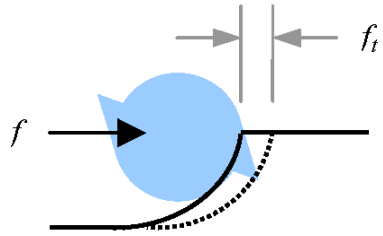

2.4 Milling process calculations/measurements

This group consists of calculations and measurements used to describe the milling process. They are based on previous decisions, experiments, and the design information and include force model identification (included as a separate uncertainty node for the purposes of this paper), Frequency Response Function (FRF) determination, process stability model, SLE model, tool life model, and the surface roughness calculation. In the decision analytic view, these calculations/measurements represent the uncertainties and the deterministic nodes in the diagram.

2.4.1 Force Model Coefficients (FMC)

A cutting force model for milling is described in equations (2) and (3) where, for each tooth in contact with the workpiece, F_t is the tangential force component, F_r is the radial force component, k_{tc} is the tangential cutting force coefficient, k_{rc} is the radial cutting force coefficient, k_{te} is the tangential edge coefficient, k_{re} is the radial edge coefficient, and h is the instantaneous chip thickness (Altintas, 2000). The value of h is a function of cutter angle, ϕ as shown in Figure 7. It can be approximated as $h = f_t \sin(\phi)$. The cutting force coefficients in milling are specific to the tool geometry-workpiece material and can also be a function of spindle speed. The forces are shown in Figure 8.

$$F_t = k_{tc} bh + k_{te} b \tag{2}$$

$$F_r = k_{rc} bh + k_{re} b. \tag{3}$$

Figure 7 Chip thickness, h, variation with cutter angle, ϕ (see online version for colours)

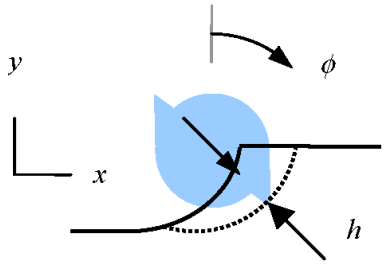

Figure 8 End milling forces; up and down milling cases are also identified (see online version for colours)

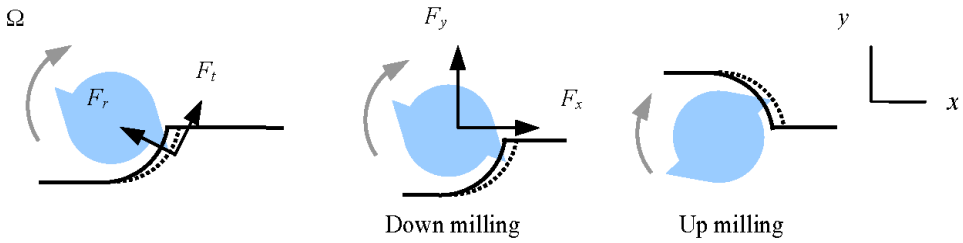

Cutting force models may be

- developed by transformation of orthogonal cutting parameters such as shear angle, shear stress, and friction coefficient to the geometry in question
- obtained from previously tabulated data; or
- determined from mechanistic identification.

Because the cutting coefficients are a function of both the workpiece material and cutting tool characteristics (as well as the cutting conditions in some cases), the mechanistic approach is often applied (Altintas, 2000).

The FMC will be treated as uncertain in this paper. To incorporate uncertainty for any random variable, X, in this analysis, we use classic probability encoding techniques for a three-degree discrete random variable. We choose three values of X, which we denote as X_{High}, X_{Base}, and X_{Low}, that represent the 90%, 50% and 10% fractiles on the cumulative probability distribution. Next, we defined a discrete probability mass function for X using the values $\{X_{\text{High}}, X_{\text{Base}}, X_{\text{Low}}\}$ with corresponding probabilities {0.25, 0.5, 0.25}. For more information on this approach see McNamee and Celona (2001); for more information on assessing probability distributions, see Spetzler and von Holstein (1975). Finally, for more information on constructing probability distributions using discrete probability assessments of the variable see Abbas (2002, 2005, 2006) and for information on constructing distributions using moments of a variable, see Smith (1993).

2.4.2 Frequency Response Function (FRF)

The FRF of a tool-holder-spindle-machine assembly is a compact means of expressing the complex-valued relationship between a harmonic force (input) and the tool point vibrations (output) in the frequency domain. In general, the FRF is recorded using impact testing, where an instrumented hammer is used to excite the tool point and the response is measured using an appropriate transducer (often a low-mass accelerometer). Schmitz et al. (2001a, 2001b), Schmitz and Donaldson (2000) and Schmitz and Duncan (2005) have also investigated modelling approaches for determining the tool point FRF. The FRF will be assumed deterministic given the tool selection for this study; provided the FRF is measured for the selected cutting tool, we believe its uncertainty contribution is small compared to FMC and tool life. However, FRF uncertainty will be considered in future work following the analysis presented by Kim and Schmitz (2007).

2.4.3 Tool life

Chip formation is primarily a shearing action. The sheared chip flows over the rake face of the cutting edge and leaves the freshly machined surface. Rubbing between the cutting edge relief face and machined surface can also occur. Due to this intimate contact between the chip and tool under high pressures at elevated temperatures, the tool tends to wear over time. There are a number of mechanisms for this wear (e.g., attrition, abrasion, adhesion and diffusion), which can take a number of forms (e.g., flank, crater and notch wear) (Tlusty, 2000). The typical approach to quantifying tool life is to pick a wear form and a maximum allowable value (such as 0.3 mm of flank wear) and perform tests to determine how long it takes to reach this value as a function of the process parameters. The time of cutting before this limit is reached is referred to as the tool life and it depends on the cutting conditions. This dependence is usually described empirically using a Taylor-type tool life equation (Taylor, 1906). An example is provided in equation (4), where the tool life, T, is described as a function of cutting surface speed, v, feed per tooth, and the constants, C, p, and q. To determine the tool life equation coefficients, cutting tests are performed (for a particular tool-workpiece pair) over a range of process parameters and the time to reach the pre-selected wear value is recorded for each combination.

$$T = Cv^{-p} f_t^{-q}, \quad \text{where } v = \frac{\pi d \cdot \Omega}{60} \text{ and } \Omega \text{ is expressed in rpm.} \tag{4}$$

Any number of process parameters can be included in the tool life model. However, cutting speed is usually one of these parameters. Because the temperature at the tool-chip interface tends to increase with cutting speed, diffusion-based wear accelerates with higher cutting speeds. This often places an upper bound on the maximum allowable cutting speed. Tool life is assumed uncertain in this paper; even under well-controlled experimental conditions, it generally exhibits a distribution in the results. We investigate the effect of incorporating uncertainty in tool life on the milling parameters (decisions).

2.4.4 Surface roughness

Surface roughness values are typically supplied with engineering drawings of the part in question. Various statistics, such as average roughness or R_a, are used to describe the smoothness of the machined surface. Theoretical limits on the milled surface smoothness are imposed by the height of the cusps left by the rotating tool path (see Figure 9). Surface roughness may be approximated using equation (5) where the plus sign is used for up milling and the minus sign is used in down milling (Alauddin et al., 1995). Surface roughness will be assumed deterministic, given tool selection and machining parameter decisions. Again, we believe its uncertainty contribution to be small relative to tool life and FMC.

$$R_a = \frac{f_t^2}{32\left(\frac{d}{2} \pm \frac{f_t N}{\pi}\right)}. \tag{5}$$

Figure 9 Illustration of surface roughness: the spacing between the cylinders represents the feed per tooth (exaggerated); the cusp heights limit the surface smoothness (see online version for colours)

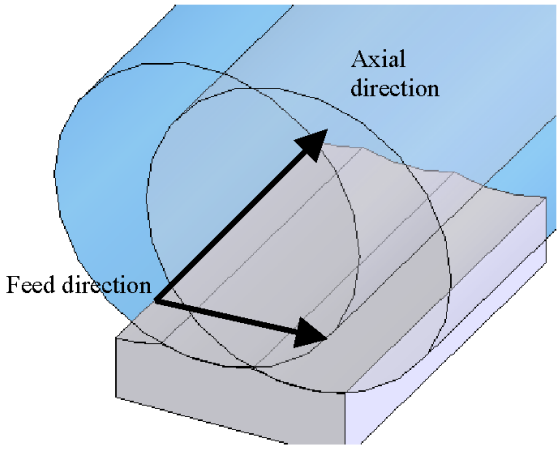

2.4.5 Process stability

Early work by Arnold (1946), Tobias (1965), Tobias and Fishwick (1958a, 1958b), Merrit (1965), Tlusty and Polocek (1963) and Koenisberger and Tlusty (1967) led to a fundamental understanding of regeneration of waviness, or the cutting of a wavy surface by a vibrating cutter, as a primary feedback mechanism for the growth of self-excited vibrations (or chatter). The cutting force applied to the tool by the chip formation process causes the tool to vibrate. These vibrations are imprinted on the work surface. When the next tooth encounters this wavy surface, the instantaneous chip thickness varies. The cutting force depends on chip thickness, so the force is modulated. This force variation affects the resulting vibration and a closed loop system is produced (the time between teeth represents the delay in the set of time-delayed differential equations that can be used to describe this system). Stable cutting conditions are achieved when the vibrations from one tooth to the next tend to copy one another (or are in phase) and the chip thickness does not vary substantially. Significant chip thickness variation can lead to chatter, exhibited as self-excited vibrations which occur at the dominant natural frequency of the dynamic system.

The phasing is determined by the spindle speed and the axial depth of cut acts as the gain in the closed loop control system (for a fixed radial depth). The stability information for the milling system can be summarised in a stability lobe diagram; Tlusty et al. (1983), Altintas and Budak (1995) and Budak, and Altintas (1998) have presented frequency-domain, analytical solutions. In this diagram, axial depth is plotted along the vertical axis and spindle speed along the horizontal axis. Stable and unstable zones are separated by the stability boundary, where any {axial depth, spindle speed} pair above the boundary leads to chatter and any pair below the boundary yields stable cutting conditions (see Figure 10). The stability boundary will be assumed deterministic using the approach described by Altintas and Budak (1995). A brief summary of the algorithm implemented in this research is provided in the Appendix.

Figure 10 Stable and unstable milling conditions are summarised in a stability lobe diagram

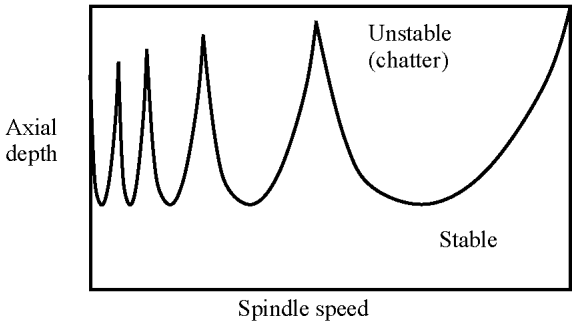

2.4.6 Surface Location Error (SLE)

Milling is, by definition, an interrupted cutting process in which the teeth on the cutting tool repeatedly impact the part and cut away small chips from the material. Therefore, even under stable cutting conditions, the tool experiences periodic forced vibrations. The magnitude and phase of these vibrations depend on the process parameters, such as the dynamic response of the system (represented by the FRF), the excitation frequency (which depends on the spindle speed and the number of teeth on the cutter), the cutting FMC, the radial and axial depths of cut, the feed per tooth, and the cutter helix angle. The location of the individual teeth as they enter (up milling) or exit (down milling) the cut as the tool vibrates determines the final location of the machined surface or SLE. Depending on the excitation frequency and its relationship to the system natural frequencies, the tool may remove less material than commanded (undercutting) or more material than commanded (overcutting). Figure 11 shows an example of undercutting SLE. SLE is assumed deterministic, given tool selection and machining parameter decisions, for the purposes of this paper. Details of SLE predictions are also included in the Appendix.

Figure 11 Surface Location Error (SLE) example (undercut) (see online version for colours)

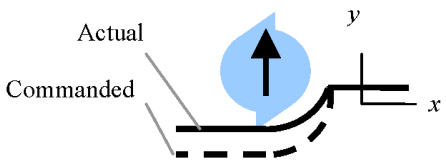

2.5 Tool path

The tool path is determined using a digital representation of the work-piece, tool-holder, fixturing, and spindle-machine (especially required for five-axis milling). The Computer Aided Design/Computer Aided Manufacturing (CAM/CAD) software prescribes the machine axis motions required to produce the desired geometry. For selected cutting depths and tool velocity profiles, the total machining time, t_m, and cutting time, t_c, can be determined from the tool path defined in the CAD/CAM software. Machining time is the total time required for the machining operation; cutting time is the fraction of machining time that the tool actually spends in the cut.

2.6 Profit calculations

2.6.1 Profit

Profit is simply the difference between revenue and cost,

$$P = R - C. \tag{6}$$

Revenue is the product of price and the number of units sold. Cost, however, can have many inputs, which may be categorised into fixed and variable costs. Fixed costs include, for example, building and machinery depreciation, insurance, taxes, interest, indirect labour, engineering, rentals, general supplies, management expenses, and marketing/sales. Examples of variable costs are materials, tooling, labour, utilities/power, and maintenance. Cost considerations specific to machining include: setup time, part quality, Computer Numerical Control (CNC) programming, inspection, cycle time, rework, finishing, part handling, fixturing, coolant use and disposal, and tool advance-retract-change times, among others (Stephenson and Agapiou, 1997). We now discuss in more detail the calculations required to determine cost, revenue, and profit.

2.6.2 Machining cost

Machining cost per part, C_m, is defined in equation (7) (Tlusty, 2000):

$$C_m = t_m r_m + (t_{ch} r_m + C_t)\frac{t_c}{T}, \tag{7}$$

where r_m is the cost to operate the machine per unit time, t_{ch} is the tool changing time, C_t is the cost per tool, and T is the tool life as determined by equation (4), for example. For simplicity, we have assigned the same cost per unit time, r_m, to both the machining and tool changing times, although we recognise that this may be over-simplified in the situation that a single machinist is tending multiple machines, for example. The machining cost per part must be multiplied by the number of units to be sold, n, and summed with the fixed costs, C_f, to arrive at the final cost, C; see equation (8). This node contains the machining cost per unit time, tool-changing time, cost per tool, number of units, and fixed costs required for the calculations in equations (7) and (8).

$$C = C_f + nC_m. \tag{8}$$

2.6.3 Revenue

This node contains the number of parts to be sold and selling price for each part. Their product defines the revenue, R.

3 Numerical case study

In this section we describe four optimisation examples for a pre-selected dynamic system, workpiece material, Taylor-type tool life model, and cutting force model. The tool point FRF was determined from a fixed-free 10 mm diameter, 42 mm long carbide beam model (550 GPa modulus, 14500 kg/m^3 density, 0.0015 solid damping coefficient) (Bishop and Johnson, 1960). This was selected for convenience to provide simple stability behaviour

(i.e., a single bending vibration mode defined the system dynamics) and is not required in general. For the tool life description, we applied the data presented by Tsai et al. (2005) for machining SKD61 tool steel using a TiAlN-coated, tungsten carbide endmill (10 mm diameter, four teeth) to generate a Taylor-type model of the form shown in equation (9), where T is expressed in min, v in m/min, f_t in mm/tooth, and b in mm. From the 42 tests using various v, f_t, and b values, the Taylor-type tool life equation coefficients were determined by least squares fitting.

$$T = 1.9549 \times 10^6 v^{-16265} f_t^{-0.1024} b^{-0.2837}. \tag{9}$$

To provide a point of comparison for our optimisation results, we first calculated the minimum cost associated with machining away a cube of the selected tool steel with a side dimension of 100 mm using the parameters suggested by a cutting tool manufacturer. Because manufacturer recommendations were not available for the exact tool-workpiece combination used in Tsai et al. (2005), we selected an equivalent tool from Sandvik Coromant. This enabled us to use their recommended cutting conditions.[1] Sandvik Coromant solid carbide tools with approximately the same coating as the tool specific by Tsai et al. (2005) have a grade designation GC1630 and the closest available geometry was provided by an R216.34-10045-AC22N tool (Sandvik Coromant, 2004, p.A148). The SKD61 tool steel corresponds to an ISO CMC No. P03.11 high-alloy steel. Additionally, cutting force coefficients for the high-alloy steel were given as $k_{tc} = 2395$ N/mm^2 and $k_{rc} = 718$ N/mm^2 (the edge coefficients were taken to be zero) (Tsai et al., 2005). The manufacturer-recommended cutting conditions for the selected tool-workpiece combination (Sandvik Coromant, 2004, p.A303) were $v = 88.5$ m/min, $f_t = 0.027$ mm/tooth, and $\Omega = 2817$ rpm (for $d = 10$ mm), where a correction factor of 1.18 was applied to obtain the recommended spindle speed corresponding to the SKD61 material hardness (Sandvik Coromant, 2004, p.A321).

$$t_m = \frac{L}{f} \tag{10}$$

$$t_c = \frac{L_c}{f} = \frac{L_c}{L} t_m \tag{11}$$

$$L = \frac{W}{b}\left(\frac{2W}{a}(W+d)+W\right) \tag{12}$$

$$L_c = \frac{W}{b}\left(\frac{W}{a}(W+d)\right). \tag{13}$$

For our optimisation study, we discretised the decision node values as shown in Table 1; seven values for each of the four decision parameters yielded a total of 2401 potential operating points. In order to determine the minimum cost associated with the manufacturer-recommended spindle speed and feed per tooth, we constructed a stability lobe diagram for each of the possible radial depths of cut. These diagrams were then used to select the allowable depth of cut (without chatter) at the 2817 rpm spindle speed. Once the candidate combinations of radial depth, feed per tooth, axial depth, and spindle speed were known, the associated tool life for each was calculated using equation (9) (the tool changing time, cost per tool, and cost to operate the machine per unit time were

taken to be 4 s, \$114, and \$1/min, respectively; no fixed costs were considered). Next, the machining and cutting times for the 100 mm cube were determined using equations (10) and (11), respectively, where L is the total length of the tool path, and L_c is the actual length of cut. See equations (12) and (13), where $W = 100$ mm is the cube side length. The down milling tool path was defined as shown in Figure 12. Given this information, the minimum cost was found to be \$808.48. In the subsequent four optimisation scenarios, the single part revenue was assumed to be equal to this cost in the current profit calculation ($P = R - C$). Therefore, any positive profit value indicates the improvement over the manufacturer-recommended operating parameters. For example, if the profit value were \$808.48, then a 100% improvement would have been achieved.

Table 1 Discretised decision variables

a (mm)	f_t (mm/tooth)	b (mm)	Ω (rpm)
2.0	0.01	1.0	23,000
2.5	0.03	1.5	25,667
3.0	0.05	2.0	28,333
3.5	0.07	2.5	31,000
4.0	0.09	3.0	33,667
4.5	0.11	3.5	36,333
5.0	0.15	4.0	39,000

Figure 12 Part path for machining the cube of dimension $W = 100$ mm; this path is repeated in multiple levels as required by the discretised axial depth of cut

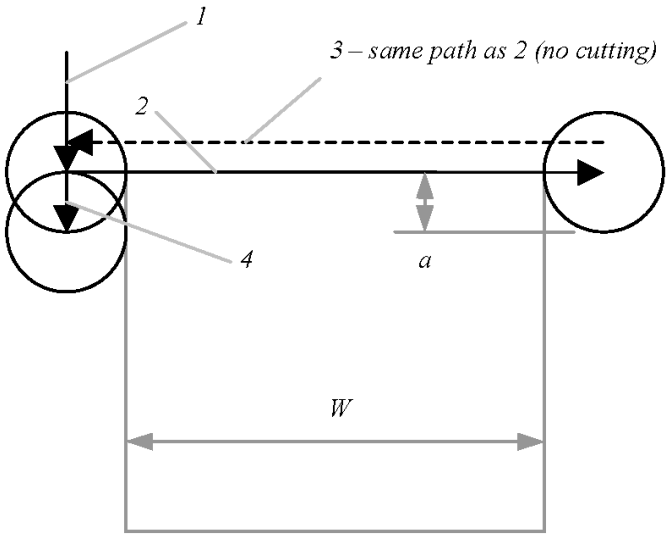

3.1 Optimisation 1: deterministic

For the first optimisation example, the deterministic problem was solved. Here, the maximum profit operating point (from the 2401 potential points) was selected using the following constraints

- the operating point was stable (no chatter)
- the absolute value of the SLE was less than or equal to 50 µm
- $R_a \leq 1$ µm.

A maximum profit of \$762.23 was obtained for the parameter set $\{a, f_t, b, \Omega\}$ of {4.5 mm, 0.15 mm/tooth, 2 mm, 36,333 rpm}.

The stability lobe diagram with superimposed profit contours (\$) and operating points for the $a = 4.5$ mm, $f_t = 0.15$ mm/tooth case is provided in Figure 13. The corresponding SLE contours (µm) are shown in Figure 14. In both cases, the infeasible points (i.e., those that violated one or more of the pre-selected constraints) are represented as solid circles, while the feasible points are shown as open diamonds and the optimum as an open star.

Figure 13 Stability lobe diagram for deterministic optimisation ($a = 4.5$ mm, $f_t = 0.15$ mm/tooth): lines of constant profit (\$) are included; the infeasible operating points are identified as solid circles; feasible points are open diamonds; and the optimum is an open star (see online version for colours)

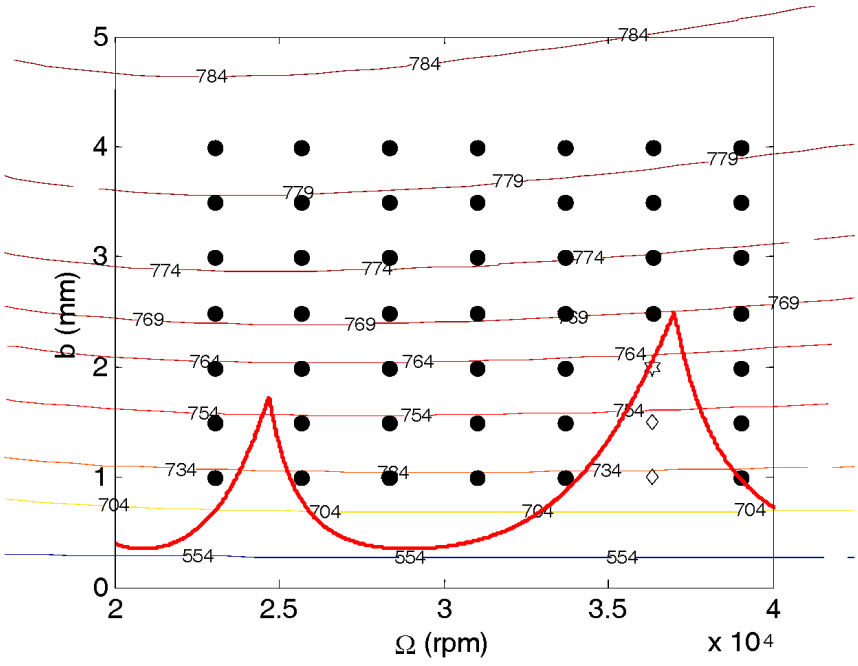

Figure 14 Stability lobe diagram for deterministic optimisation (a = 4.5 mm, f_t = 0.15 mm/tooth) with superimposed Surface Location Error (SLE) contours (μm) (see online version for colours)

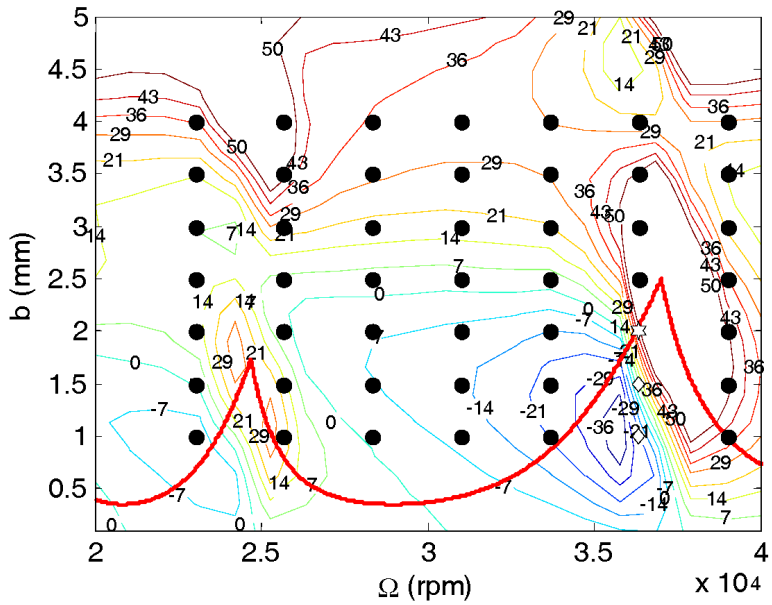

3.2 Optimisation 2: uncertain force model

In this case, the tool life was assumed deterministic and the FMC, k_{tc} and k_{rc}, were encoded to specify the different degrees of the uncertainty. The High-Base-Low values for the FMC (F_{High}, F_{Base}, and F_{Low}, respectively) were obtained by direct assessment. For each of the High-Base-Low force model coefficient values we then calculated the optimal profit.

We assumed a symmetric distribution and encoded a Base k_{tc} value of 700 N/mm^2 (typical for aluminum alloys) to obtain a corresponding symmetric variation increment of 150 N/mm^2 for Low and High. This increment was then linearly scaled to the actual k_{tc} mean (Base) value of 2395 N/mm^2. The Low and High k_{rc} values maintained the same proportionality as the mean k_{rc} value to the mean k_{tc} value. This approach was taken because the direct assessment subject had more experience with aluminum than tool steel.

For variation in the FMC, two of the selected constraints, stability and SLE, were potentially affected. Higher coefficients tend to reduce the stability limit and increase the absolute value of SLE. Therefore, the constraints were evaluated for each operating point three times – once for each of the encoded force model coefficient sets. For each of these 2401 × 3 evaluations, a binary multiplier value, $M(F, S)$, was assigned, where F is the degree of the force model coefficient, {High-Base-Low}, and S represents the settings. The multiplier value was 1 if no constraints were violated and 0 otherwise. The expected profit, $E[P(T, S)]$, was calculated for each of the 2401 × 3 points as shown in equation (14). Here the $P(T_{\text{Base}}, S)$ value, obtained from the deterministic tool life analysis, was used because variations in FMC do not affect the profit calculation – only the constraints (i.e., they may change feasibility). Because the tool life is deterministic in this case, we set tool life to its median value, T_{Base}.

$$E[P(T,S)] = P(T_{\text{Base}},S)\{0.25\times M(F_{\text{Low}},S)+0.5 \times M(F_{\text{Base}},S)+0.25\times M(F_{\text{High}},S)\}. \quad (14)$$

The optimum profit of \$751.45 for this case was obtained for {a, f_t, b, Ω} equal to {3 mm, 0.15 mm/tooth, 2.5 mm, 36333 rpm}. The stability lobe diagram (a = 3 mm) variation with coefficient values and profit curves (\$) are provided in Figure 15. In this diagram, the upper stability limit corresponds to the Low force coefficients and 14 feasible points are shown (open diamonds). However, a number of these points are stable for only the Base and/or Low force coefficient values. For example, the lower left point is unstable for the High force coefficient values. This leads to an $M(F_{\text{High}}, S)$ value of 0 in equation (14) and a significantly reduced expected profit at this potential operating point. The reader may note that the introduction of new uncertainties does not always lead to significant change in the optimal decision, as shown in the next section.

Figure 15 Stability lobe diagram for uncertain force model optimisation (a = 3 mm, f_t = 0.15 mm/tooth): three stability limits are shown; they correspond to the low (upper dashed line), mean (middle solid), and high coefficient values (lower dashed); lines of constant profit (\$) are also included; the infeasible operating points are identified as solid circles, feasible points are open diamonds, and the optimum is an open star (see online version for colours)

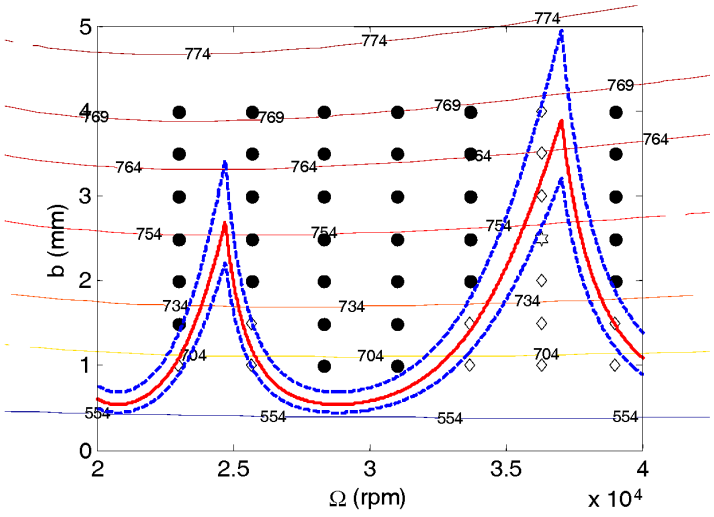

3.3 *Optimisation 3: uncertain tool life*

In this case, the tool life was assumed uncertain while the FMC were considered deterministic. The deterministic tool life value obtained from equation (9) (based on the selected operating point) was varied over three discrete values using the results of an encoding exercise similar to that described for the FMC. The three values were T_{Low}, T_{Base}, and T_{High}, where T_{Base} is the deterministic value of tool life we used in Section 3.2. The expected profit was then determined as:

$$E[P(T,S)] = M(F_{\text{Base}},S)\{0.25\times P(T_{\text{Low}},S) +0.5\times P(T_{\text{Base}},S)+0.25\times P(T_{\text{High}},S)\}. \quad (15)$$

Tool life variation does not impact the constraints (for the model assumptions applied here), so the feasible points are identical to the deterministic case. The expected profit for each point was calculated according to equation (15) and the optimum profit was \$761.84 for the same operating conditions as the deterministic case (Section 3.1). The close agreement between these two results is explained using Figure 16. This figure shows that, even though the tool life uncertainty leads to different profit curves, the symmetry in the variation yields an expected profit curve that is very close to the profit based on the mean tool life. In future studies, we will evaluate whether a symmetric tool life distribution is appropriate. For example, DeGarmo et al. (2003, p.539) suggest that a log normal tool life distribution is preferred. Other future analyses will also include sensitivity to the chosen High-Base-Low values and their effect on expected profit.

Figure 16 Profit vs. spindle speed for a = 4.5 mm, f_t = 0.15 mm/tooth, b = 2 mm: the upper and lower dashed lines correspond to the highest and lowest encoded tool life values, respectively; the solid line represents the mean tool life profit and the dotted line the expected profit (equation (15)) (see online version for colours)

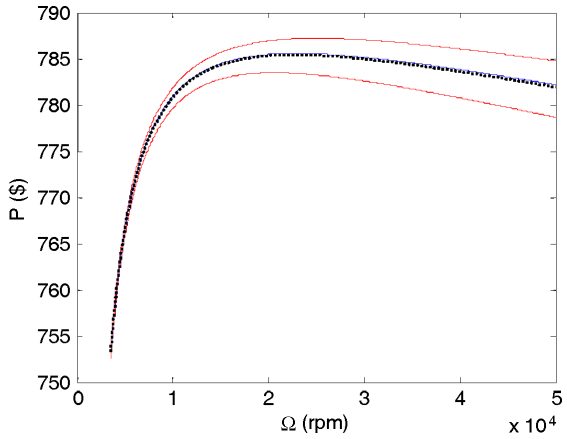

3.4 Optimisation 4: uncertain tool life and force model

In this situation we considered both the FMC and tool life and to be uncertain and applied the encoded values described in Sections 3.2 and 3.3, respectively. The calculation for the new expected profit is provided in equation (16). As anticipated, the optimum profit of \$750.95 is close to the uncertain force model case and occurs at the same operating point, {3 mm, 0.15 mm/tooth, 2.5 mm, 36333 rpm}. This is again due to the symmetry in the profit curves about the Base (mean) value for the encoded tool life (see Figure 16).

$$E(P(T,S)) = (0.25\times M(F_{\text{Low}},S) + 0.5\times M(F_{\text{Base}},S) + 0.25\times M(F_{\text{High}},S)) \times (0.25\times P(T_{\text{Low}},S) + 0.5\times P(T_{\text{Base}},S) + 0.25\times P(T_{\text{High}},S)). \quad (16)$$

The optimisation results for the four cases are summarised in Table 2. The reader may note that, even for the lowest profit from the final case, the cost savings over the manufacturer-recommended conditions is 93% (i.e., a profit value of \$750.95 represents a cost of \$57.53, given the revenue value of \$808.48 based on the cost determined from the manufacturer-recommended conditions).

Table 2 Summary of optimisation results

Optimisation	a (mm)	f_t (mm/tooth)	b (mm)	Ω (rpm)	*Profit* ($)
Deterministic	4.5	0.15	2.0	36333	762.23
Tool life uncertain	4.5	0.15	2.0	36333	761.84
Force model uncertain	3.0	0.15	2.5	36333	751.45
Tool life and force model uncertain	3.0	0.15	2.5	36333	750.95

3.5 Tornado diagrams

As mentioned in Section 3.2, different uncertainties have varying effects on the optimal milling parameters (decisions). Tornado diagrams provide a means to quickly identify those uncertainties that contribute most significantly to the overall variance in the value model. A tornado diagram varies one uncertainty across its Low-Base-High values and keeps the remaining uncertainties fixed at their base values. In each case, we then calculate the profit for each instantiation of these values and plot it as a horisontal bar. The same is repeated for all other uncertainties varying across their Low-Base-high values. For our model, we selected particular milling parameter decisions and plotted the tornado diagrams; see Figure 17. It is seen that the bars corresponding to FMC are indeed much wider than those corresponding to the Tool Life (TL) variation, showing that the uncertainty contributed by tool life in this example is much less than that contributed by FMC.

Figure 17 Tornado diagrams for selected operating points $\{a, f_t, b, \Omega\}$: (a) {2 mm, 0.05 mm/tooth, 1.0 mm, 20,000 rpm}; (b) {2 mm, 0.05 mm/tooth, 4.0 mm, 10,000 rpm}; (c) {2 mm, 0.19 mm/tooth, 1.0 mm, 10,000 rpm} and (d) {3 mm, 0.19 mm/tooth, 2.5 mm, 18,333 rpm} (see online version for colours)

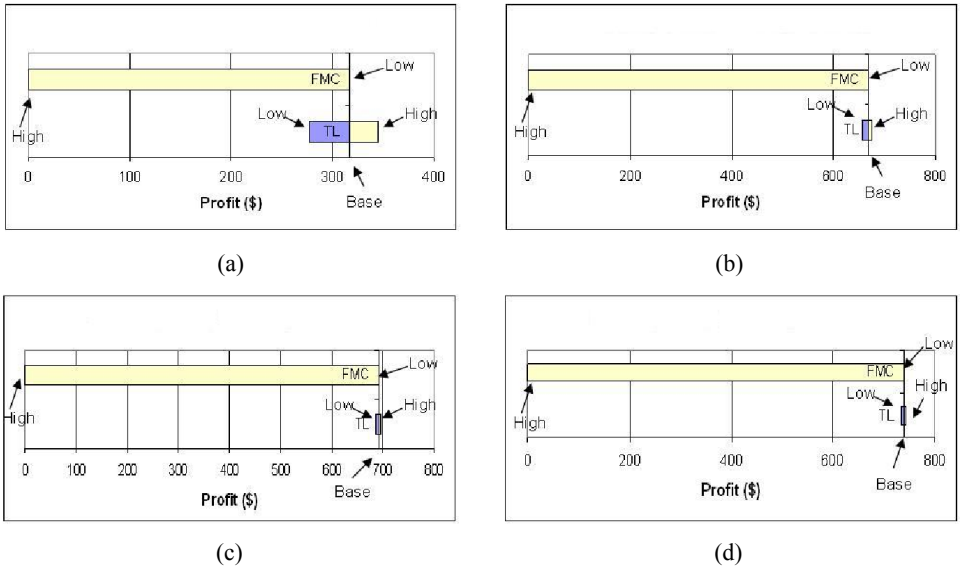

4 Conclusions

This study described initial steps in the application of decision analysis to milling optimisation. We first identified the decision diagram for milling considering the influence of the process dynamics (stability and (SLE)), surface roughness, and tool life on profit optimisation. Next, we completed a numerical study of four optimisation scenarios

- deterministic
- uncertainty in the force model only
- uncertainty in tool life only
- uncertainty in both the force model and tool life.

It was shown that the optimised expected profit was not strongly sensitive to tool life uncertainty, but this was due to the symmetric nature of the tool life variation. In practice, a symmetric distribution may not fully reflect experiment; further, the tool life and force coefficients were considered independent, which may not be an acceptable assumption. It was also shown that uncertainty in the FMC yielded a different optimum with lower expected profit than the deterministic case. Finally, it was demonstrated that the optimised result for all four cases was considerably more profitable than what would be obtained by cutting parameters recommended by the tool manufacturer for a test case.

Acknowledgements

The authors gratefully acknowledge financial support for this work from the National Science Foundation (DMI-0642569 and DMI-0641827). They also wish to thank G. Hazelrigg for numerous helpful discussions and insights and M. Kurdi and R. Haftka for their contributions to the case study.

References

Abbas, A.E. (2002) 'Entropy methods for univariate distributions in decision analysis', *23rd International Workshop on Bayesian Inference and Maximum Entropy Methods in Science and Engineering*, Moscow.

Abbas, A.E. (2005) 'Maximum entropy distributions between upper and lower bounds', *25th International Workshop on Bayesian Inference and Maximum Entropy Methods in Science and Engineering*, San Jose, CA.

Abbas, A.E. (2006) 'Entropy methods for joint distributions in decision analysis', *IEEE Transactions on Engineering Management*, Vol. 53, No. 1, pp.146–159.

Alauddin, M., El Baradie, M.A. and Hashmi, M.S.J. (1995) 'Computer-aided analysis of a surface roughness model for end milling', *Journal of Materials Processing Technology*, Vol. 55, pp.123–127.

Altintas, Y. (2000) *Manufacturing Automation*, Cambridge University Press, Cambridge, UK.

Altintas, Y. and Budak, E. (1995) 'Analytical prediction of stability lobes in milling', *Annals of the CIRP*, Vol. 44, No. 1, pp.357–362.

Armarego, E.J.A., Smith, A.J.R. and Wang, J. (1993) 'Constrained optimization strategies and CAM software for single-pass peripheral milling', *International Journal of Production Research*, Vol. 31, No. 9, pp.2139–2160.

Armarego, E.J.A., Smith, A.J.R. and Wang, J. (1994) 'Computer-aided constrained optimization analyses and strategies for multi-pass helical tooth milling operations', *Annals of the CIRP*, Vol. 43, No. 1, p.437.

Arnold, R.N. (1946) 'The mechanism of tool vibration in the cutting of steel', *Proceedings of the Institution of Mechanical Engineers*, Vol. 154, No. 4, pp.261–284.

Beightler, C.S. and Philips, D.T. (1970) 'Optimization in tool engineering using geometric programming', *AIIE Transactions*, Vol. 2, pp.355–360.

Bishop, R.E.D. and Johnson, D.C. (1960) *The Mechanics of Vibration*, Cambridge University Press, Cambridge.

Boothroyd, G. and Rusek, P. (1976) 'Maximum rate of profit criteria in machining', *ASME Journal of Engineering for Industry*, Vol. 98, pp.217–220.

Budak, E. and Altintas, Y. (1998) 'Analytical prediction of chatter stability conditions for multi-degree of freedom systems in milling, part I, modeling, part II, applications', *Journal of Dynamic Systems, Measurement and Control*, Vol. 120, pp.22–36.

DeGarmo, E., Black, J. and Kohser, R. (2003) *Materials and Processes in Manufacturing*, 9th ed., Wiley and Sons, Inc., Hoboken, NJ.

Deshayes, L., Welsch, L., Donmez, A. and Ivester, R. (2005) 'Robust optimization for Smart Machining Systems, an enabler for agile manufacturing', *Proceedings of American Society of Mechanical Engineers International Mechanical Engineering Congress and Exposition*, IMECE2005-81537, Orlando, FL.

Ermer, D. (1971) 'Optimization of the constrained machining economics problem by geometric programming', *ASME Journal of Engineering for Industry*, Vol. 93, pp.1067–1072.

Eskicioglu, H., Nisli, M.S. and Kilic, S.E. (1985) 'An application of geometric programming to single-pass turning operations', *Proceedings of the International MTDR Conference*, Birmingham, pp.149–157.

Giardini, C., Bugini, A. and Pagagnella, R. (1988) 'The optimal cutting conditions as a function of probability distribution function of tool life and experimental test numbers', *International Journal of Machine Tools and Manufacture*, Vol. 28, pp.453–459.

Gilbert, W. (1950) 'Economics of machining', *Machining – Theory and Practice*, American Society for Metals, Metals Park, OH, pp.465–485.

Gopalakrishnak, B. and Al-Khayyal, F. (1991) 'Machine parameter selection for turning with constraints, An analytical approach based on geometric programming', *International Journal of Production Research*, Vol. 29, pp.1897–1908.

Hati, S.K. and Rao, S.S. (1976) 'Determination of optimum machining conditions – deterministic and probabilistic approaches', *ASME Journal of Engineering for Industry*, Vol. 98, pp.354–359.

Howard, R.A. and Matheson, J.E. (1984) 'Influence diagrams', in Howard, R.A. and Matheson, J.E. (Eds.): *The Principles and Applications of Decision Analysis*, Strategic Decisions Group, Menlo Park, CA, Vol. II, pp.627–639.

Howard, R.A and Matheson, J.E. (2005) 'Influence diagrams', *Decision Analysis*, Vol. 2, No. 3, pp.127–143.

Jha, N.K. (1990) 'A discrete database multiple objective optimization of milling operation through geometric programming', *Journal of Engineering for Industry*, Vol. 112, p.368.

Juan, H., Yu, S.F. and Lee, B.Y. (2003) 'The optimal cutting-parameter selection of production cost in HSM for SKD61 tool steels', *International Journal of Machine Tools and Manufacture*, Vol. 43, pp.679–686.

Keefer, D., Kirkwood, C. and Corner, J. (2004) 'Perspective on decision analysis applications, 1990–2001', *Decision Analysis*, Vol. 1, No. 1, pp.4–22.

Kim, K-K., Kang, M-C., Kim, J-S., Jung, Y-H. and Kim, N-K. (2002) 'A study on the precision machinability of ball end milling by cutting speed optimization', *Journal of Materials Processing Technology*, Vols. 130–131, pp.357–362.

Kim, H.S. and Schmitz, T. (2007) 'An investigation of uncertainty in impact testing', *Proceedings of the International Conference on Smart Machining*, 13–15 March, Gaithersburg, MD, (on CD).

Koenisberger, F. and Tlusty, J. (1967) *Machine Tool Structures–Vol. I*, *Stability against Chatter*, Pergamon Press, London, UK.

Lambert, B.K. and Walvekar, A.G. (1978) 'Optimization of multipass machining operations', *International Journal of Production Research*, Vol. 9, pp.247–259.

Lin, T-R. (2002) 'Optimization technique for face milling stainless steel with multiple performance characteristics', *International Journal of Advanced Manufacturing Technology*, Vol. 19, pp.330–335.

Lu, J., Ozdoganlar, O.B., Kapoor, S.G. and DeVor, R.E. (2003) 'A process-model based methodology for comprehensive process planning of contour turning operations', *Transactions of NAMRI/SME*, Vol. XXXI, pp.547–554.

McNamee, P. and Celona, J. (2001) *Decision Analysis for the Professional*, 3rd ed., SmartOrg Inc., Menlo Park, CA.

Merrit, H. (1965) 'Theory of self-excited machine tool chatter', *Journal of Engineering for Industry*, Vol. 87, No. 4, pp.447–454.

Okushima, K., and Hitomi, K. (1964) 'A study of economic machining, an analysis of the maximum-profit cutting speed', *International Journal of Production Research*, Vol. 3, No. 1, pp.73–78.

Petropoulos, P.G. (1975) 'Optimal selection of machining rate variables by geometric programming', *International Journal of Production Research*, Vol. 13, pp.390–395.

Sandvik Coromant (2004) *Rotating Tools and Inserts Handbook*, LIT-CAT 04-R.

Schmitz, T., Davies, M. and Kennedy, M. (2001a) 'Tool point frequency response prediction for high-speed machining by RCSA', *Journal of Manufacturing Science and Engineering*, Vol. 123, pp.700–707.

Schmitz, T., Davies, M., Medicus, K. and Snyder, J. (2001b) 'Improving high-speed machining material removal rates by rapid dynamic analysis', *Annals of the CIRP*, Vol. 50, No. 1, pp.263–268.

Schmitz, T. and Donaldson, R. (2000) 'Predicting high-speed machining dynamics by substructure analysis', *Annals of the CIRP*, Vol. 49, No. 1, pp.303–308.

Schmitz, T. and Duncan, G.S. (2005) 'Three-component receptance coupling substructure analysis for tool point dynamics prediction', *Journal of Manufacturing Science and Engineering*, Vol. 127, No. 4, pp.781–790.

Schmitz, T. and Mann, B. (2006) 'Closed form solutions for surface location error in milling', *International Journal of Machine Tools and Manufacture*, Vol. 46, pp.1369–1377.

Sheikh, A.K., Kendall, L.A. and Pandit, S.M. (1980) 'Probabilistic optimization of multitool machining operations', *ASME Journal of Engineering for Industry*, Vol. 102, pp.239–246.

Smith, J.E. (1993) 'Moment methods for decision analysis', *Management Science*, Vol. 39, No. 3, pp.340–358.

Sonmez, A.I., Baykasoglu, A., Turkay, D. and Filiz, I.H. (1999) 'Dynamic optimization of multi-pass milling operations via geometric programming', *International Journal of Machine Tools and Manufacture*, Vol. 39, No. 2, pp.297–320.

Spetzler, C.S. and von Holstein, C.S. (1975) 'Probability encoding in decision analysis', *Management Science*, Vol. 22, pp.340–358.

Stephenson, D. and Agapiou, J. (1997) *Metal Cutting Theory and Practice*, Marcel Dekker, Inc., New York, NY.

Tansel, I., Ozcelik, B., Bao, W., Chen, P., Rincon, D., Yang, S. and Yenilmez, A. (2006) 'Selection of optimal cutting conditions by using GONNS', *International Journal of Modeling and Simulation*, Vol. 46, No. 1, pp.26–35.

Taylor, F.W. (1906) 'On the art of cutting metal', *Transactions of the ASME*, Vol. 28, p.31.

Tee, L, Ho, S. and DeVries, M. (1969) *Economic Machining Charts*, ASTME Paper No. MR pp.69–280.

Tlusty, J. (2000) *Manufacturing Processes and Equipment*, Prentice-Hall, Inc., Upper Saddle River, NJ.

Tlusty, J. and Polocek, M. (1963) 'The stability of the machine-tool against self-excited vibration in machining', *Proceedings of the International Research in Production Engineering Conference*, Pittsburgh, PA, p.465.

Tlusty, J., Zaton, W. and Ismail, F. (1983) 'Stability lobes in milling', *Annals of the CIRP*, Vol. 32, No. 1, pp.309–313.

Tobias, S.A. (1965) *Machine-Tool Vibration*, Blackie and Sons Ltd., Glasgow, Scotland.

Tobias, S.A. and Fishwick, W. (1958a) 'The chatter of lathe tools under orthogonal cutting conditions', *Transactions of the ASME*, Vol. 80, p.1079.

Tobias, S.A. and Fishwick, W. (1958b) 'Theory of regenerative machine tool chatter', *The Engineer*, London, p.205.

Tsai, M.K., Lee, B.Y. and Yu, S.F. (2005) 'A predicted modeling of tool life of high speed milling for SKD61 tool steel', *International Journal of Advanced Manufacturing Technology*, Vol. 26, p.711.

Walvekar, A.G. and Lambert, B.K. (1970) 'An application of geometric programming to machining variable selection', *International Journal of Production Research*, Vol. 8, pp.241–245.

Wang, J. and Armarego, E.J.A. (2001) 'Computer-aided optimization of multiple constraint single pass face milling operations', *Machining Science and Technology*, Vol. 5, No. 1, pp.77–99.

Wu, S.M. and Ermer, D. (1966) 'Maximum profit as the criterion in the determination of the optimum cutting conditions', *ASME Journal of Engineering for Industry*, Vol. 88, pp.435–442.

Note

[1]Note that the recommended cutting parameters may be conservative in nature and were not suggested to be an optimum solution by Sandvik Coromant.

Appendix: Milling process models

In the Altintas and Budak (1995) milling stability algorithm, the time varying coefficients of the dynamic milling equations, which depend on the angular orientation of the cutter as it rotates through the cut, are expanded into a Fourier series and then truncated to include only the average component. The stability analysis is posed as an eigenvalue problem similar to the form det $(A - \lambda I) = 0$, where λ represents the system complex eigenvalues, I is the identity matrix, and A is defined in equation (A1), where $G_{x/y}$ and $H_{x/y}$ are the real and imaginary parts of the tool point FRFs in the x and y directions, respectively. The terms α_{xx}, α_{xy}, α_{yx}, and α_{yy} depend on the selected radial immersion and the cutting force coefficient, $K_r = k_{rc}/k_{tc}$.

$$A = \begin{bmatrix} \alpha_{xx}(G_x + iH_x) & \alpha_{xy}(G_y + iH_y) \\ \alpha_{xy}(G_x + iH_x) & \alpha_{yy}(G_y + iH_y) \end{bmatrix}. \tag{A1}$$

The resulting stability relationships are shown in equations (A2)–(A4), where $b_{\lim}$ is the limiting axial depth of cut without chatter, ω_c is the chatter frequency (should it occur), and j is an integer ($j = 0, 1, 2, \ldots$). The reader may note that these equations differ slightly from those in Altintas and Budak (1995) because the eigenvalue problem formulation has been slightly modified.

$$b_{\lim} = \frac{2\pi \cdot \mathrm{Re}(\lambda)}{Nk_{tc}(\mathrm{Re}(\lambda)^2 + \mathrm{Im}(\lambda)^2)}\left(1 + \left(\frac{\mathrm{Im}(\lambda)}{\mathrm{Re}(\lambda)}\right)^2\right) \tag{A2}$$

$$\Omega = \frac{\omega_c}{N}\frac{1}{(\gamma + 2\pi \cdot j)} \tag{A3}$$

$$\gamma = \pi - 2 \cdot \tan^{-1}\left(\frac{\mathrm{Im}(\lambda)}{\mathrm{Re}(\lambda)}\right). \tag{A4}$$

The analytical, frequency domain solution for SLE applied here requires two assumptions (Schmitz and Mann, 2006). First, the influence of regeneration is neglected because the machining process is stable and governed by steady state vibrations. Second, although tool vibrations occur in both the x and y directions, y direction vibrations dominate the surface location (for x direction feed). Given these conditions, the solution method can be divided into three steps:

- express the y direction cutting force in the frequency domain
- determine the y direction displacement in the frequency domain by multiplying the y direction cutting force by the y direction FRF

$$Y(\omega) = \frac{Y(\omega)}{F_y(\omega)} F_y(\omega) \tag{A5}$$

- inverse Fourier transform the resulting displacement data and sample at the cut entrance (for up milling) or exit (down milling) to determine SLE.